Using Multi-Angle Implementation of Atmospheric Correction (MODIS) to characterize anisotropy in the Amazonian forests

Yhasmin Mendes de Moura [1]
Thomas Hilker [2]
Lenio Soares Galvao [1]
Joao Roberto dos Santos [1]
Alexei Lyapustin [3]
Celio Helder de Sousa Resende [2]

[1] Instituto Nacional de Pesquisas Espaciais - INPE
Caixa Postal 515 - 12227-010 - São José dos Campos - SP, Brasil
{yhasmin, lenio, jroberto}@dsr.inpe.br

[2] Oregon State University - OSU
97331 - Corvallis - OR, United States
{thilker, celio.sousa}@oregonstate.edu

[3] Goddard Space Flight Center - NASA
20771 - Greenbelt - MD, United States
alexei.i.lyapustin@nasa.gov

Abstract. The objective of this work is to present initial results of a new method to evaluate vegetation patterns in the Amazon rainforests based on multi-angle satellite observations. We used MODIS Enhanced Vegetation Index (EVI) data processed by MAIAC algorithm to generate anisotropy, calculated by the differences between hotspot and darkspot reflectance. We compared Anisotropy with EVI using two images (June 2008), both processed by MAIAC, to demonstrate the potential of using anisotropy for mapping vegetation structure of different forests types. We also analyzed seasonal variability between anisotropy and EVI, and compared our findings with variability of monthly water deficit for the region. Finally, we discussed the use of anisotropy to infer spatial-temporal changes in vegetation structure. The results showed larger spatial variability of anisotropy, while EVI varied only to a limited extend across the study area. The regional differences in anisotropy may therefore better represent the structural heterogeneity across forested areas in the Amazon, based on the interaction of vegetation with multi-angle scattering. Seasonal changes were more gradual when using Anisotropy compared to using EVI. This gradient transition across months is in good agreement with water deficit patterns derived from the Tropical Rainfall Measurement Mission (TRMM). Our study hypothesizes that multiangular information are useful sources to analyze structural changes in different types of forests, and may provide new opportunities to monitor tropical forests, from optical remote sensing.

Key-words: Anisotropy, MODIS, MAIAC, EVI, Amazon, Anisotropia, MODIS, MAIAC, EVI, Amazônia.

1. Introduction

The response of tropical forests to climate change has received great attention by the scientific community due to the important role that this vegetation plays in the global carbon, water and energy cycle. For instance, the Amazonian rainforests account for about 15% of global photosynthesis and host about a quarter of the world's terrestrial species (Malhi et al., 2008). Within the last 10 years the Amazon basin has experienced two severe droughts, one in 2005 and other in 2010 (Marengo et al., 2011). Several studies had indicated that tropical forests are sensitive to droughts with significant consequences for carbon loss due to fire and tree mortality (Aragao et al., 2007; Asner et al., 2004; Meir et al., 2008).

Loss of forest productivity across Amazonia as a result of change in precipitation patterns would clearly exacerbate global climate change. Satellite-remote sensing is the major source of knowledge to observe climate sensitivity of Amazon vegetation and ecosystem dynamics at useful spatial and temporal scales (Asner and Alencar, 2010). However, the effect of such changes on tropical vegetation is still largely unknown. Remote sensing investigations based on Moderate Resolution Imaging Spectroradiometer (MODIS)'s Enhanced Vegetation Index (EVI), have been controversial regarding the vegetation status in Amazônia. For instance, Saleska et al. (2007) reported an increase in greenness for the 2005 drought, whereas Xu et al., 2011, observed a widespread decline in photosynthetic activity for the 2010 drought. Also, Phillips et al., 2009, estimated that the severe Amazon drought in 2005 resulted in a total carbon loss of about 1.2-1.6 Pg. Samanta et al. (2010) suggested deficiencies in estimation of atmospheric aerosol loadings and cloud screening over tropical regions as cause for these conflicting evidences. According to Atkinson et al. (2011), local climate factors (e.g., reduced cloud cover) or noise-related factors (e.g., erros of atmospheric correction) may have contributed to inter-annual MODIS variability in EVI.

One of the fundamental challenges for optical remote sensing of canopy characteristics is the dependence of these measurements on extraneous effects such as soil background and the observation geometry (Kempeneers et al., 2008). For instance, canopy level estimates of biophysical parameters from spectral vegetation indices are strongly affected by the viewing and solar geometry (Galvao et al., 2011; Moura et al., 2012).

The Multi-Angle Implementation of Atmospheric Correction (MAIAC) is a new generation cloud screening and atmospheric correction algorithm for MODIS data that uses an adaptative time series analysis and processing of group of pixels to derive atmospheric aerosol concentration and surface reflectance without typical empirical assumptions. Previous research has shown reductions in noise by a factor of up to 10, in addition MAIAC also yields more cloud free observations (Hilker et al., 2012). The algorithm implements a time series of multi-day observations to provide sufficient information for simultaneous retrievals of atmospheric aerosol and surface bidirectional reflectance distribution function (BRDF) (Lyapustin et al., 2011, 2012).

Consequently, MAIAC provides new opportunities to investigate changes in vegetation cover based on multi-angle information acquired from forward and backscatter observations and may therefore allow us to detect more subtle changes in vegetation to seasonal patterns. Such multi-angle observations provide a means to characterize the anisotropy of surface reflectance (Chen et al., 2005), which contains information on the structure of vegetated surfaces and shaded parts of the canopy (Chen et al., 2003, Gao et al 2003).

The objective of this work is to present new methods to evaluate vegetation patterns in the Amazon rainforests based on multi-angle satellite observations. We used MODIS Enhanced Vegetation Index (EVI) data processed by MAIAC algorithm to generate anisotropy, calculated by the differences between forward and backscatter modeled by the bi-directional reflectance distribution function. We analyzed the potential of multi-angular information from satellite imagery (Anisotropy) compared with the conventional EVI product. We also discuss use of anisotropy to infer spatial-temporal changes in vegetation structure.

2. Methods

2.1 Approach

MAIAC data were processed for 12 MODIS tiles including all the Amazon rainforest (h10v08 to h13v10, spanning 10^0N to 20^0S in latitude and 80^0 W to 42^0W in longitude) from NASA's Level 1 and Atmosphere Archive and Distribution System (LAADS Web)

ftp://ladsweb.nascom.nasa.gov/MAIAC. MAIAC is based on MODIS Collection 6 Level 1B (calibrated and geometrically corrected) observations, which removes major sensor calibration degradation effects present in earlier collections. First, we show the improvements of the MAIAC compared to the conventional BRDF MODIS product (MCD43A4) . We used two EVI images (June 2008), both processed by MAIAC, to demonstrate the differences between the EVI and the Anisotropy. Areas with difference types of forests were compared. We also analyzed seasonal variability between anisotropy and EVI, and compared with monthly water deficit variability for the region. Estimates of Water Deficit (WD) were acquired between January 2000 and December 2012 from the Tropical Rainfall Measuring Mission (TRMM), product 3B43 version 7, at 0.25º spatial resolution. The WD is based on the assumption that a moist tropical forest transpires about 100 mm.month[-1] (Anderson, 2012). Consequently, the forest is considered stressed when rainfall goes below 100 mm.month[-1].
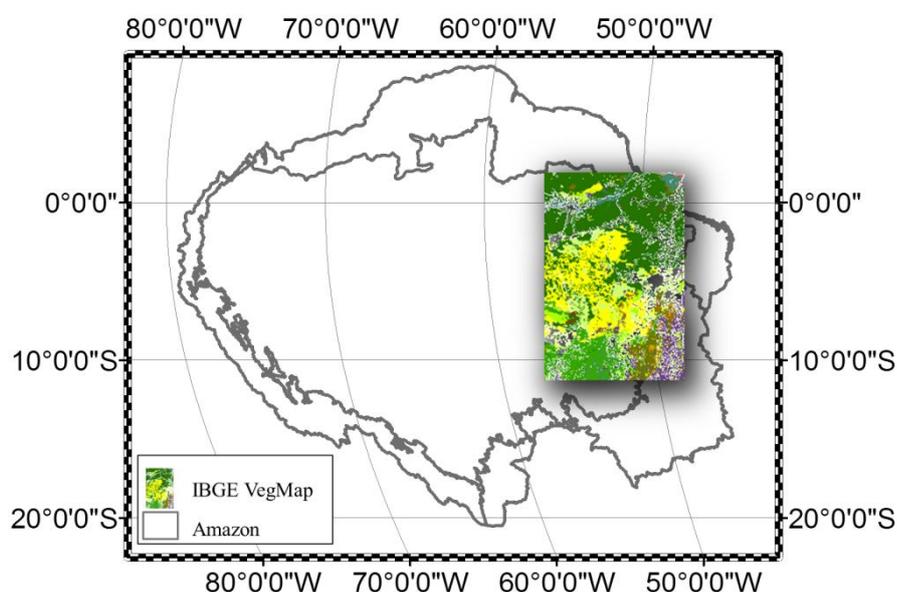

Figure 1. Study area (Amazon) and the indicated vegetation map (IBGE, 2004) used for the comparison analysis.

2.2 MAIAC algorithm

The MAIAC algorithm grids MODIS L1B data to a 1 km resolution, and accumulates measurements of the same surface area from different orbits (view geometries) for up to 16 days using a moving window approach. The cloud mask (CM) algorithm composes a dynamically updated reference clear-sky image of the surface from spatial and time series analyses. The knowledge of reference clear-sky reflectance in addition to spectral and thermal reflectance tests (Ackerman et al., 1998) has been shown to improve cloud detection (Lyapustin et al., 2008). MAIAC aerosol retrieval (Lyapustin et al., 2011) and atmospheric correction (Lyapustin et al., 2012) algorithms use an advanced radiative transfer theory with anisotropic land surface reflectance (Lyapustin and Knyazikhin, 2001) parameterized by the Ross-Thick Li-Sparse (RTLS, Wanner and Strahler., 1995) bidirectional reflectance model (Lyapustin et al., 2011). In our study, the Ross-Thick and Li-Sparse kernel functions (Roujean et al., 1992) were used based on the radiative transfer theory of Ross (1981) and the geometric-optical model of Li and Strahler (1986):

$$\rho(\theta_v,\theta_s,\Delta\phi) = k_i + k_g K_L(\theta_v,\theta_s,\Delta\phi,\tfrac{h}{b},\tfrac{b}{r}) + k_v K_R(\theta_v,\theta_s,\Delta\phi) \qquad \text{(Eq. 1)}$$

Where:

k_i	isotropic scattering component
k_g	geometric scattering component
K_L	Li-Sparse kernel
k_v	volumetric scattering component
K_R	Ross-Thick kernel
θ_v	view zenith angle (VZA)
θ_s	solar zenith angle (SZA)
$\Delta\phi$	relative azimuth angle (RAA)
$\frac{h}{b}$	crown relative height =1 (Wanner et al., 1995, Justice et al., 1998)
$\frac{b}{r}$	crown relative shape =2 (Wanner et al., 1995, Justice et al., 1998)

k_i, k_g and k_v are the empirical components (kernel weights) and were derived from mathematical inversion of the linear model using the MODIS reflectance observations. Once k_i, k_g and k_v are acquired, ρ can be obtained for any view observer geometry by setting $\theta_v, \theta_s, \Delta\phi$. The use of BRDF model rather than provided reflectance allows us to maintain constant sun-observer geometry for the back- and forward scatter observations.

Our analysis is based on the EVI calculated as:

$$EVI(\theta_v, \theta_s, \Delta\phi) = G \times \frac{\rho_{nir(\theta_v, \theta_s, \Delta\phi)} - \rho_{red(\theta_v, \theta_s, \Delta\phi)}}{\rho_{nir(\theta_v, \theta_s, \Delta\phi)} + C_1 \times \rho_{red(\theta_v, \theta_s, \Delta\phi)} - C_2 \times \rho_{blue(\theta_v, \theta_s, \Delta\phi)} + L} \qquad \text{(Eq. 2)}$$

Where:
$\rho(\theta_v, \theta_s, \Delta\phi)$ is the atmospherically corrected surface reflectance for a give sun sensor geometry;
L is the canopy background adjustment (1.0);
C1 (6.0) and C2 (7.5) are the coefficients of the aerosol resistance term;
G (2.5) is a scaling factor (Huete et al., 1994).

Reflectance anisotropy can be characterized as the difference of reflectance hotspot (SZA=45°, VZA=45°, RAA=180°) and darkspot (SZA=45°, VZA=45°, RAA= 0°), computed from the BRDF model. The anisotropy were calculated as the difference between backscatter and forwardscatter images:

$$Anisotropy_{EVI} = EVI_{backscatter} - EVI_{forwardscatter} \qquad \text{(Eq. 3)}$$

3. Results and Discussion

From a statistical standpoint, the ability to detect change in vegetation depends on the number of observations available and the noise inherent in the reflectance product. Figure 2 shows a comparison of available high quality pixels for the BRDF corrected product, we are comparing the MAIAC algorithm and the conventional MODIS MCD43A4 product (NBAR - nadir BRDF-adjusted reflectance). The black line represent the MAIAC product, and the grey line represent the product MCD43A4. The number of valid observations (based on the proportion of cloud free and high quality pixels) for MAIAC were about 2 to 5 times higher than for the MCD43A4 product (Hilker et al., 2012). It should be noted that NBAR is a composite product, using 16 day of observations, which explains part of the difference in

available observations. Even though MAIAC is based on all available pixels as opposed to best pixel mosaicking, Hilker et al. (2012) showed that uncertainties of MAIAC are by a factor of 1-2 lower compared to the conventional product. In conclusion, both, the number of available pixels and noise levels in existing observations should enhance the ability of MAIAC to detect changes in vegetation cover. The remainder of this study focuses on comparison between mono-angle approaches as typically implemented using vegetation indices and multi-angle anisotropy for detecting seasonal and spatial changes in vegetation cover.
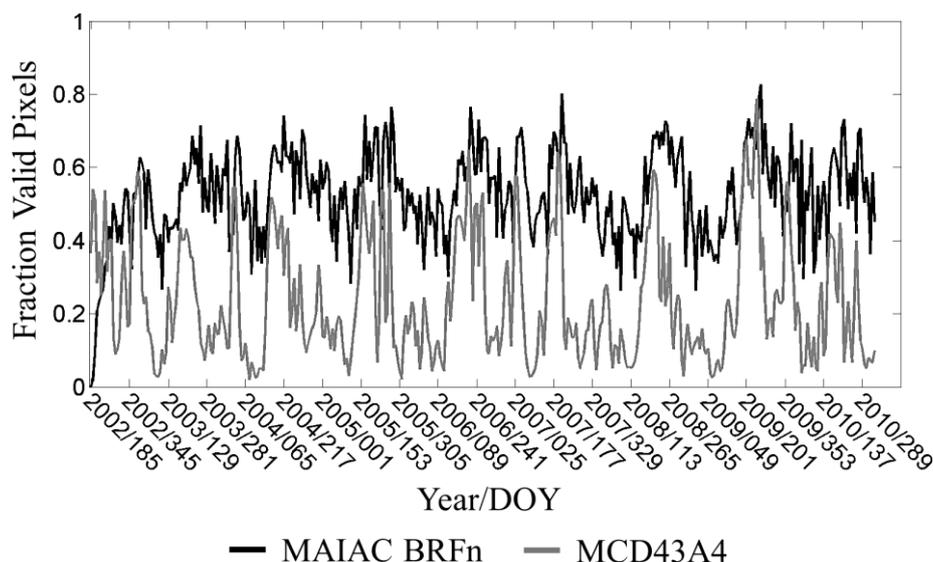

Figure 2. (adapted from Hilker et al., 2012) Comparison between available high quality pixels in MAIAC data and MCD43A4 data. Note that MAIAC observations is daily, while MCD43A4 is 16 days composite.

Figure 3 shows a comparison between EVI and Anisotropy for the Amazon basin. EVI was obtained from MCD13 16 day composites, anisotropy was calculated from daily BRDF's using MAIAC. The upper part of Figure 3 shows a dry season mean of EVI (left side) and anisotropy (right side). The selected (highlighted) area consists of different vegetation cover types, as shown by the vegetation cover map (IBGE, 2004) included in a section of the figure. Main vegetation types include dense Ombrophilous, open Ombrophilous and semi-deciduous forest. Spatial variability of the conventional EVI is presented on the left, while anisotropy is shown on the right. The figure demonstrates a larger spatial variability of anisotropy, while EVI varied only to a limited extend across the study area. Our study hypothesizes that the sensibility in the Anisotropy in represent different vegetation cover types is due the interaction of the vegetation with multi-angle scattering. In contrast, EVI is non-linearly related to leaf area, and as a result, tends to saturate in dense vegetation types.
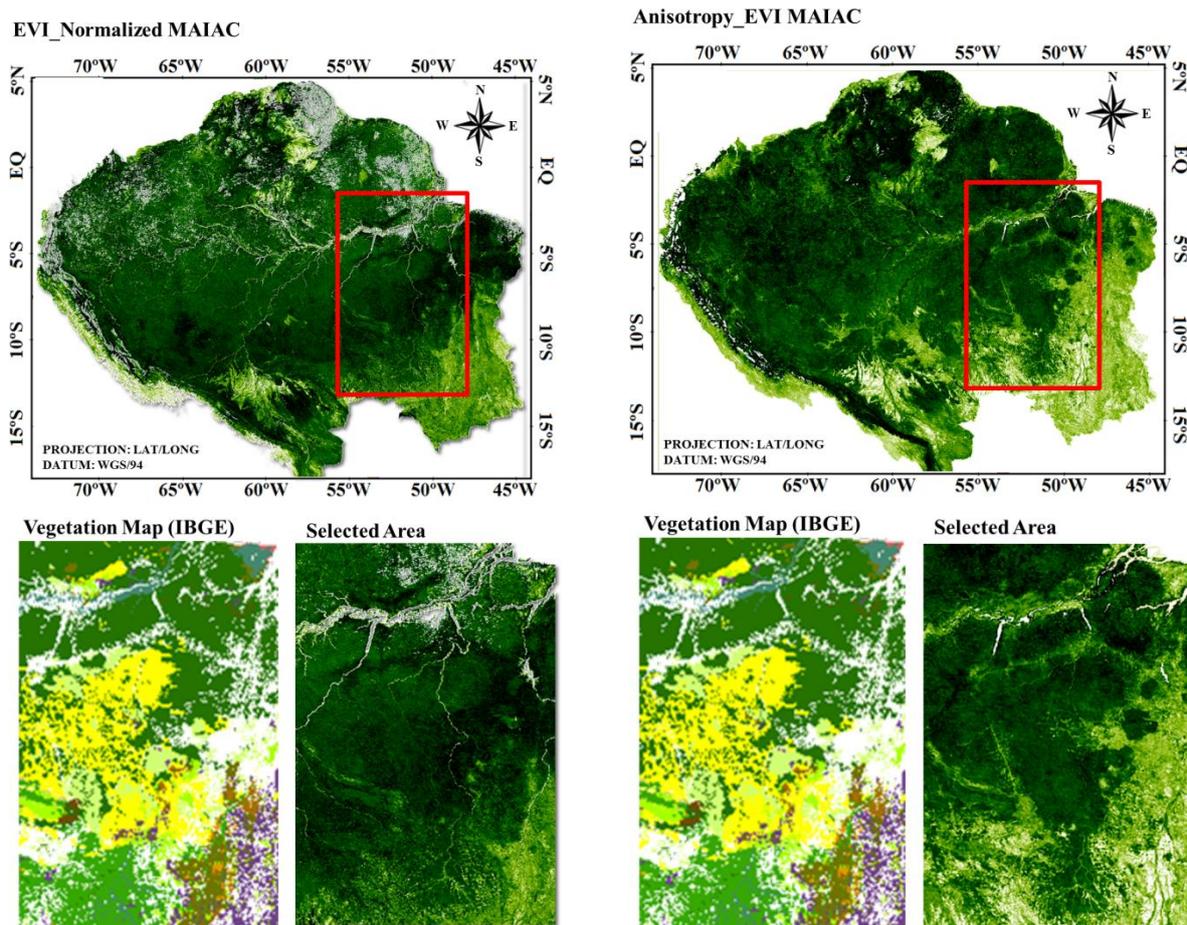
Figure 3. Comparison of EVI (left side) and anisotropy (right side) obtained from multi-angle scattering of EVI using MAIAC. The upper figure shows a comparison across the Amazon basin, the lower maps demonstrate a focus area including a vegetation type map to illustrate the different vegetation types found in the region.

A seasonal analysis of patterns in EVI and Anisotropy is illustrated in Figure 4. The figure largely confirms the findings of Figure 3 and demonstrates the ability of anisotropy to depict structural variability also in the temporal domain. Seasonality (dry and wet season) can vary substantially across the Amazon region, for instance, the southern regions are typically more seasonal than the central area of the basin. Figure 4 illustrates large seasonal swings in the anisotropy product, while results based on EVI showed more distinct differences in the south eastern region only during the month of July. It can also be seen from our analysis that the anisotropy presented these seasonal changes much more gradually when compared with the EVI. This gradient transition across months is in good agreement with the water deficit patterns found in this area and demonstrated in Figure 5. The Figure illustrates the high seasonal variation and the spatial variability in the water availability, given the monthly maps of water deficit in the region. Two seasonal patterns could be detected, as shown by the high levels of water deficit in the extreme north area for the months Jan to Apr, related to the dry season in the north hemisphere, and, May to Aug, in the south hemisphere.
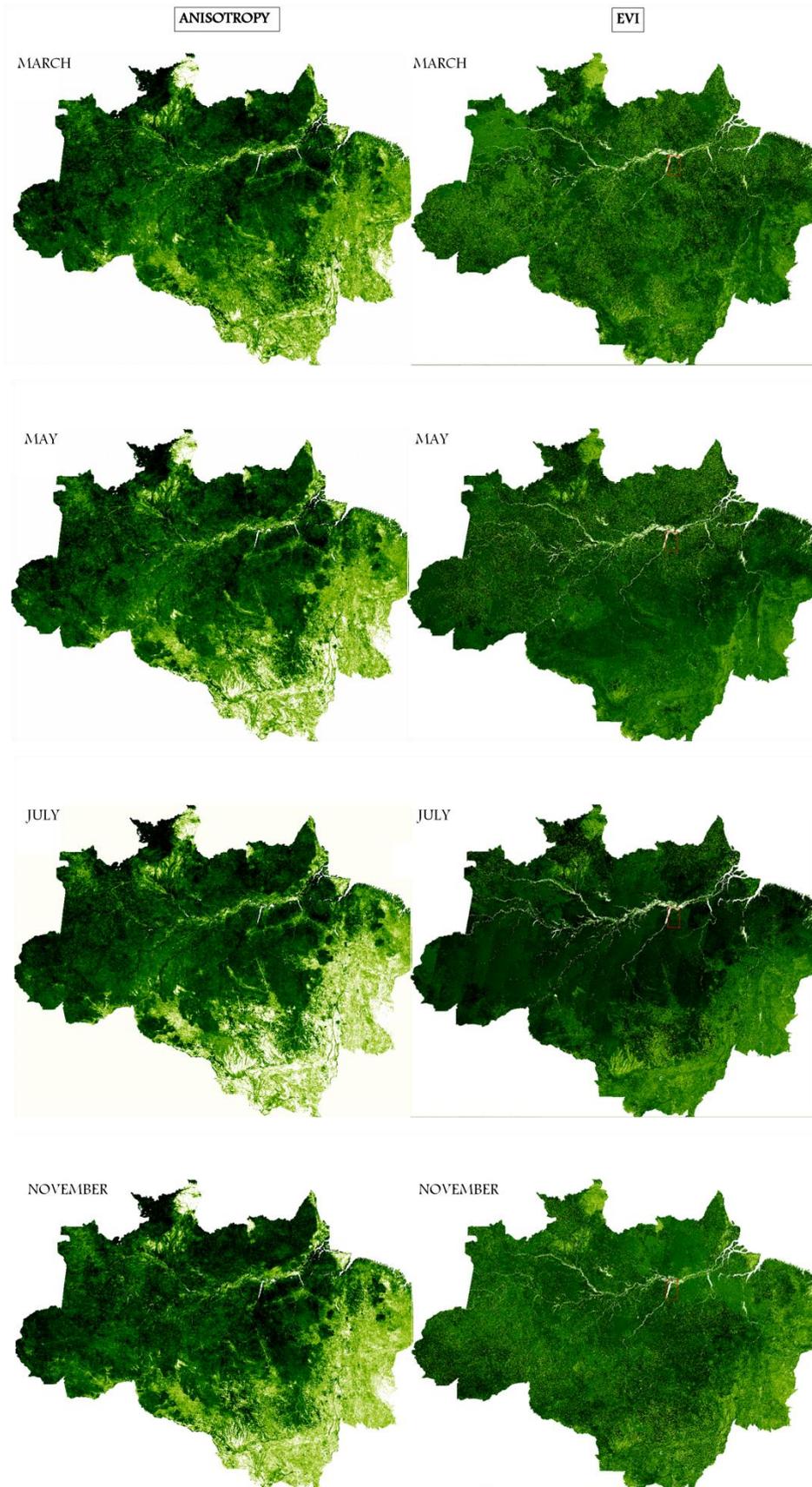
Figure 4: Seasonal variability in anisotropy (left side) and EVI (right side). The figure illustrates the more pronounced seasonal variability in Anisotropy which is in good agreement with water availability demonstrated in Figure 5.
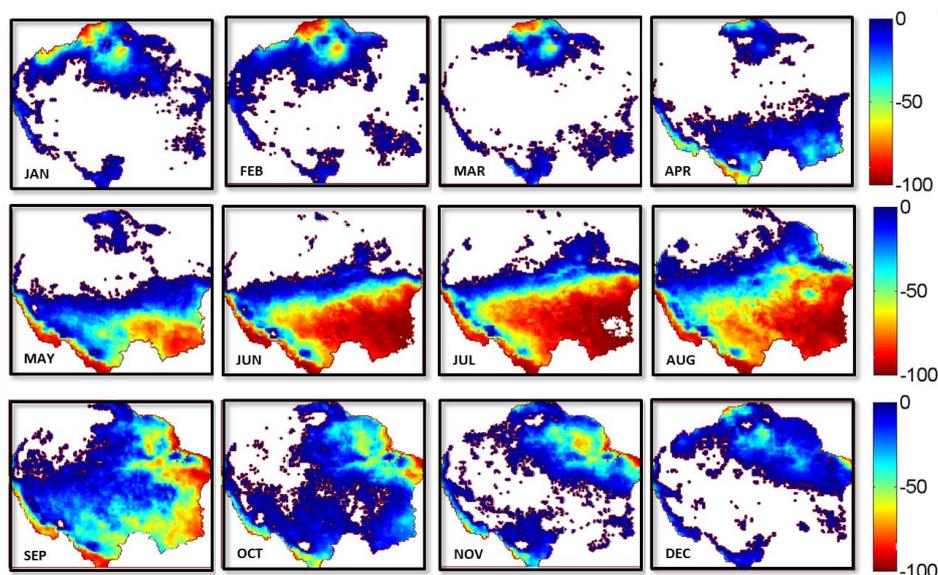
Figure 5. Water deficit based on the TRMM dataset for the Amazon region considering the period 2000 to 2012.

4. Conclusions

This study presented initial results based on the comparative analysis between the EVI and Anisotropy to show a new multi-angle approach to monitor the vegetation status in tropical regions from MODIS data. This study is a simple demonstration of the potentials of these product (Anisotropy) to observe spatial variability between forests within the Amazon. We conclude that novel data processing techniques such as MAIAC provide new opportunities to leverage multi-angle information of existing satellite data and may therefore provide a more comprehensive understanding of the spatio-temporal patterns in Amazon vegetation cover.

Acknowledgements

References

Ackerman, S. A., Strabala, K. I., Menzel, W. P., Frey, R. A., Moeller, C. C., & Gumley, L. E. (1998). Discriminating clear sky from clouds with MODIS. **Journal of Geophysical Research**, *103*(D24), 32141. doi:10.1029/1998JD200032

Anderson, L. O. Biome-scale forest properties in Amazonia based on field and satellite observations. **Remote Sensing**, v. 4, n.5, p. 1245-1271, 2012.

Aragão, L. E. O. C., Malhi, Y., Cuesta, R. M. R., Saatchi, S., Anderson, L. O., & Shimabukuro, Y. (2007). Spatial patterns and fire response of recent Amazonian droughts. **Geophisical Research Letters**, *34(7)*, L07701. doi: 10.1029/2006GL028946

Asner, G. P., & Alencar, A. (2010). Drought impacts on the Amazon forest: the remote sensing perspective. **The New Phytologist**, *187*(3), 569–78. doi:10.1111/j.1469-8137.2010.03310.x

Asner, G. P., Nepstad, D., Cardinot, G., & Ray, D. (2004). Drought stress and carbon uptake in an Amazon forest measured with spaceborne imaging spectroscopy. **Proceedings of the National Academy of Sciences of the United States of America**, *101*(16), 6039-6044. doi:10.1073/pnas.0400168101

Atkinson, P. M., Dash, J., & Jeganathan, C. (2011). Amazon vegetation greenness as measured by satellite sensors over the last decade. **Geophysical Research Letters**, *38*(19), n/a–n/a. doi:10.1029/2011GL049118

Chen, J. M., Liub, J., Leblanc, S. G., Lacazec, R., & Roujean, J. L. (2003). Multi-angular optical remote sensing for assessing vegetation structure and carbon absorption. **Remote Sensing of Environment**, *84(4)*, 516-525. doi: 10.1016/S0034-4257(02)00150-5

Chen, J. M., Menges, C. H., & Leblanc, S. G. (2005). Global mapping of foliage clumping index using multi-angular satellite data. **Remote Sensing of Environment**, *97*(4), 447–457. doi:10.1016/j.rse.2005.05.003

Galvão, L. S., dos Santos, J. R., Roberts, D., Breunig, F., Marcelo, B., Toomey, M., & Moura, Y. M. (2011). On intra-annual EVI variability in the dry season of tropical forest: A case study with MODIS and hyperspectral data. **Remote Sensing of Environment**, *115*(9), 2350–2359. doi:10.1016/j.rse.2011.04.035

Gao, F. (2003). Detecting vegetation structure using a kernel-based BRDF model. **Remote Sensing of Environment**, *86*(2), 198–205. doi:10.1016/S0034-4257(03)00100-7

Hilker, T., Lyapustin, A. I., Tucker, C. J., Sellers, P. J., Hall, F. G., & Wang, Y. (2012). Remote sensing of tropical ecosystems: Atmospheric correction and cloud masking matter. **Remote Sensing of Environment**, *127*, 370–384. doi:10.1016/j.rse.2012.08.035

Huete, A., Justice, C., & Liu, H. (1994). Development of vegetation and soil indices for MODIS-EOS. **Remote Sensing of Environment**, *49*(3), 224–234. doi:10.1016/0034-4257(94)90018-3

Kempeneers, P., Zarco-Tejada, P. J., North, P. R. J., de Backer, S., Delalieux, S., Sepulcre-Cantó, G., et al. (2008). Model inversion for chlorophyll estimation in open canopies from hyperspectral imagery. **International Journal of Remote Sensing**, 29(17-18), 5093–5111. doi:10.1080/01431160802036458

Li, X., Strahler, A. H. (1986). Geometric-Optical Bidirectional Reflectance Modeling of a Conifer Forest Canopy, **Geoscience and Remote Sensing**, *IEEE Transactions*, (6), 906–919.

Lyapustin, A. I., Wang, Y., Laszlo, I., Hilker, T., G.Hall, F., Sellers, P. J., et al. (2012). Multi-angle implementation of atmospheric correction for MODIS (MAIAC): 3. Atmospheric correction. **Remote Sensing of Environment**, *127*, 385–393. doi:10.1016/j.rse.2012.09.002

Lyapustin, A., & Knyazikhin, Y. (2001). Green 's function method for the radiative transfer. **Applied Optics**. *40*(21), 3495–3501.

Lyapustin, A., Wang, Y., & Frey, R. (2008). An automatic cloud mask algorithm based on time series of MODIS measurements. **Journal of Geophysical Research**, *113*(D16), D16207. doi:10.1029/2007JD009641

Lyapustin, A.I., Martonchik, J., Wang, Y., Laszlo, I., Korkin, S. (2011). Multiangle implementation of atmospheric correction (MAIAC): 1. Radiative transfer basis and look-up tables. **Journal of Geophisical Research**, *(116), D03210.* doi: 10.1029/2010JD014985

Malhi, Y., Roberts, J. T., Betts, R. A, Killeen, T. J., Li, W., & Nobre, C. A. (2008). Climate Change, Deforestation, and the Fate of the Amazon. **Science**, *319*(5860), 169-172. doi:10.1126/science.1146961

Marengo, J. A., Tomasella, J., Alves, L. M., Soares, W. R., & Rodriguez, D. A. (2011). The drought of 2010 in the context of historical droughts in the Amazon region. **Geophysical Research Letters**, *38*(12), doi:10.1029/2011GL047436

Meir, P., Metcalfe, D. B., Costa, A. C. L., & Fisher, R. A. (2008). The fate of assimilated carbon during drought: impacts on respiration in Amazon rainforests. **Philosophical Transactions of the Royal Society of London. Series B, Biological Sciences**, *363*(1498), 1849–55. doi:10.1098/rstb.2007.0021

Moura, Y. M., Galvao, L. S., dos Santos, J. R., Roberts, D. A., & Breunig, F. M. (2012). Use of MISR/Terra data to study intra- and inter-annual EVI variations in the dry season of tropical forest. **Remote Sensing of Environment**, *127*, 260–270. doi:10.1016/j.rse.2012.09.013

Phillips, O. L., Aragão, L. E. O. C., Lewis, S. L., Fisher, J. B., Lloyd, J., López-gonzález, G., et al. (2009). Drought Sensitivity of the Amazon Rainforest. **Science**, *323*(5919), 1344-1347. doi**:** 10.1126/science.1164033

Ross, I. (1981). **The radiation regime and architecture of plant stand**. Springer Science & Business Media (p. 931).

Roujean, J. L.; Leroy, M.; Deschamps, P.Y. (1992). A Bidirectional Reflectance Model of the Earth's Surface for the Correction of Remote Sensing Data, **Jornal of Geophisycal Research**, *97*(92), 455-468.

Saleska, S. R., Didan, K., Huete, A. R., & da Rocha, H. R. (2007). Amazon forests green-up during 2005 drought. **Science**, *318*(5850), 612. doi:10.1126/science.1146663

Samanta, A., Ganguly, S., Hashimoto, H., Devadiga, S., Vermote, E., Knyazikhin, Y., et al. (2010). Amazon forests did not green-up during the 2005 drought. **Geophysical Research Letters**, *37*(5), n/a–n/a. doi:10.1029/2009GL042154

Wanner, W., Li, X., & Strahler, A. H. (1995). On the derivation of kernels for kernel-driven models of bidirectional reflectance. **Journal of Geophysical Research**, *100*(D10), 21077. doi:10.1029/95JD02371

Xu, L., Samanta, A., Costa, M. H., Ganguly, S., Nemani, R. R., & Myneni, R. B. (2011). Widespread decline in greenness of Amazonian vegetation due to the 2010 drought. **Geophysical Research Letters**, *38*(7). doi:10.1029/2011GL046824